Available online at www.sciencedirect.com
SCIENCE DIRECT
Biochemical Pharmacology 70 (2005) 1613–1622
Biochemical Pharmacology
www.elsevier.com/locate/biochempharm

Inhibition of store-operated calcium entry-mediated superoxide generation by histamine trifluoromethyltoluide independent of histamine receptors

Dong-Chan Kim [a,b], So-Young Lee [a], Dong-Jae Jun [a], Sun-Hee Kim [a], Jong-Hee Lee [a], Eun-Mi Hur [a], Nam-In Baek [c], Kyong-Tai Kim [a,*]

[a] *Division of Molecular and Life Science, SBD-NCRC, Pohang University of Science and Technology, Pohang 790-784, POSTECH, San 31, Hyoja Dong, South Korea*
[b] *Division of Research and Development, Neuronex Inc., Pohang 790-784, South Korea*
[c] *Graduate School of Biotechnology & Plant Metabolism Research Center, Kyung Hee University, Suwon 449-701, Pohang 790-784, South Korea*

Received 15 August 2005; accepted 6 September 2005

Abstract

Store-operated calcium entry (SOCE) plays an important role in shaping the Ca^{2+} response of various tissues and cell types. In this report, we show that thapsigargin (TG)-induced SOCE was inhibited by the histamine receptor agonist, histamine-trifluoromethyltoluide (HTMT), in U937 and HL-60 human promyelocytes. Preincubation of HTMT resulted in a significant inhibition of subsequent TG-induced Ca^{2+} elevation without affecting Ca^{2+} release from intracellular stores. HTMT also inhibited TG-induced Ca^{2+} current and Ba^{2+}/Mn^{2+} influx in a concentration-dependent manner. In contrast with HTMT, other H1 histamine receptor agonists, histamine, 2-methylhistamine and 2-thiazolylethylamine, did not affect TG-induced SOCE. In addition, HTMT also attenuated TG-induced cytosolic superoxide generation. Taken together, our data clearly suggest that the anti-inflammatory effect of HTMT may occur through direct inhibition of SOCE.

Keywords: SOCE; Calcium; HTMT; Superoxide; Inflammation

1. Introduction

Neutrophils are the main effectors of the innate immune response through an array of microbicidal mechanisms, including chemotaxis, phagocytosis, exocytosis and generation of reactive oxygen species, leading to inflammation and host defense [1]. Increased $[Ca^{2+}]_i$ is an early cellular response during inflammation [2], and has been implicated in superoxide generation [3]. This receptor-mediated increase in cytosolic Ca^{2+} has been shown to involve two closely coupled pathways: a transient release of stored Ca^{2+}, followed by the slow entry of extracellular Ca^{2+}. The initial Ca^{2+} spike is evoked by the activation of phosphoinositide-specific phospholipase C (PLC). This enzyme hydrolyzes membrane phosphatidylinositol 4,5-bisphosphate to generate the second messenger, D-*myo*-inositol 1,4,5-trisphosphate (IP_3), which interacts with the IP_3 receptor on internal Ca^{2+} stores, releasing Ca^{2+} [4]. However, the mechanism regulating Ca^{2+} entry across the plasma membrane, which accounts for the sustained increase in $[Ca^{2+}]_i$, is still unclear. In non-excitable cells, for example, depletion of Ca^{2+} stores has been found to induce Ca^{2+} influx across the plasma membrane, referred to as store-operated calcium entry (SOCE) [5].

SOCE is a critical mechanism involved in the regulation of intracellular calcium concentration and has been found to control a wide variety of cellular functions, including cell differentiation [6], cell death [7], respiratory burst and degranulation [8]. It has been hypothesized that the empty-

Abbreviations: $[Ca^{2+}]_i$, cytosolic calcium ion concentration; Fura-2/AM, fura-2 penta acetoxymethyl ester; H_1R, histamine 1 receptor; HTMT, histamine trifluoromethyltoluide; SOCE, store-operated Ca^{2+} entry

* Corresponding author. Tel.: +82 54 279 2297; fax: +82 54 279 2199.
E-mail address: ktk@postech.ac.kr (K.-T. Kim).

0006-2952/$ – see front matter © 2005 Elsevier Inc. All rights reserved.
doi:10.1016/j.bcp.2005.09.001

ing of calcium stores may be linked to the opening of calcium entry channels through several mechanisms [5]. Some evidence has pointed to a fusion mechanism, in which the SOC channels reside in intracellular vesicles and only become integrated into the plasma membrane after the vesicles have fused with the plasma membrane. Other proposals have suggested at the probability of a direct coupling mechanism of store and plasma membrane proteins, analogous to the model of excitation–contraction coupling in skeletal muscle. Yet another scenario involves the generation of a third messenger, calcium influx factor (CIF) [9]. Regulation of SOCE has been observed in all eukaryotes, indicating that it may be a means to ensure a relatively constant concentration of Ca^{2+} in the endoplasmic reticulum, where it is required for proper protein synthesis and processing [10]. It has also been suggested that SOCE might play a more direct role in generating or modulating the Ca^{2+} oscillations, by contributing Ca^{2+} to the process of IP_3-sensitized calcium-induced calcium release [11]. The importance of SOCE is evident by the close correlation of SOCE and gene expression [12].

Despite much research on SOCE, only a few compounds have been reported to be potent SOCE inhibitors [13,14]. Histamine trifluoromethyltoluides (HTMT), a histamine receptor agonist, has been reported as a novel immunosuppressive agent [15]. Furthermore, HTMT also related with intestinal inflammation [16]. However, the effect of HTMT on SOCE-induced inflammation has not been reported. We, therefore, investigated the effect of HTMT on SOCE and SOCE-induced superoxide production and found that HTMT directly inhibits SOCE in U937 and HL-60 cells.

2. Materials and methods

2.1. Materials

Thapsigargin, cytochrome *c*, phorbol 12-myristate 13-acetate (PMA) and sulfinpyrazone were purchased from Sigma (St. Louis, MO). HTMT and mepyramine purchased from Tocris (Bristol, UK). 2-Methylhistamine and 2-thiazolylethylamine were kindly provided by GlaxoSmithKline (Hertfordshire, UK) fura-2 penta-acetoxymethyl ester (fura-2/AM), CM-H_2DCFDA were obtained from Molecular Probes (Eugene, OR). RPMI 1640, DMEM and penicillin/streptomycin were obtained from Life Technologies (Grand Island, NY). Bovine calf serum was obtained from HyClone (Logan, UT). Fetal bovine calf serum was obtained from JBI (WelGENE Inc., South Korea).

2.2. Cell culture

HL-60 cells and U937 cells were grown in RPMI 1640 supplemented with 10% (v/v) heat-inactivated bovine calf serum and 1% (v/v) penicillin/streptomycin. C6 mouse glioma cells were grown in DMEM with 10% (v/v) fetal calf serum and 1% (v/v) penicillin/streptomycin. The culture medium was changed daily. All cells were cultured in a humidified atmosphere of 95% air and 5% CO_2. We induced differentiation of the cells by incubating them in 1 μM all-*trans*-retinoic acid (trans-RA) for 5 days (HL-60 cells) [17] and in 1.25% DMSO (v/v) for 4 days or 1 μM PMA for 3 h (U937 cells) [18,19]. We counted viable cells by the trypan blue exclusion method [20].

2.3. Electrophysiology

Macroscopic currents in PMA-induced differentiated U937 cells were recorded in the whole cell configuration of the patch-clamp technique. The high Ca^{2+} extracellular solution used for store-operated Ca^{2+} current recordings containing (in mM) 130 NaCl, 20 tetraethylammonium-Cl, 10 $CaCl_2$, 1 $MgCl_2$, 5 glucose and 10 HEPES (pH adjusted to 7.4 with NaOH). Recording pipettes were made from filament borosilicate capillary glass (TW150F-6, 1.5 mm o.d., World Precision Instruments Sarasota, FL), having resistances of 2–3 MΩ. Pipette solution contained (in mM): 100 Cs-methane sulfonate, 1 $MgCl_2$, 10 HEPES and 10 EGTA (pH adjusted to 7.3 with CsOH). Membrane currents were recorded with an Axopatch 200A amplifier (Axon Instruments, Foster City, CA). Signals were obtained at sampling rates of 5 kHz and filtered at 1 kHz. The WinWCP software (written by John Dempster of Strathclyde Univ., UK) was used to control generation of stimuli and to collect data. Capacitance subtraction was done in all recordings. The series resistances were within 10 MΩ. Experiments were conducted at room temperature (20–23 °C).

2.4. Measurement of superoxide secretion

Superoxide generation was determined based on the change in absorbance of cytochrome *c* using a previously published method with slight modification [21]. Briefly, 5×10^6 cells were washed, resuspended with Locke's solution (154 mM NaCl, 5.6 mM KCl, 1.2 mM $MgCl_2$, 2.2 mM $CaCl_2$, 5 mM HEPES and 10 mM glucose, pH 7.3), and placed into a cuvette, and 40 μM cytochrome *c* was added. After a 1-min incubation, stimulants were added, and the change in absorbance at 550 nm was monitored. Superoxide dismutase was used as the control, setting the maximal value of the superoxide-mediated absorbance change. Calibration of the change in absorbance in terms of superoxide production was performed using the following equation: [superoxide] = $\Delta A v/t/K/l$ per cells, where ΔA is the change in absorbance, v the reaction volume, t the time, K the extinction coefficient for the difference between the light absorption of reduced cytochrome *c* and that of oxidized cytochrome *c* ($21 \times 10^3\ cm^{-1}\ M^{-1}$) and l is the length of the cuvette. Fluorescence of CM-H_2DCFDA, an oxidation-sensitive fluorescence probe, was also tested using a slight mod-

ification of a previously published procedure [22]. Briefly, the cell suspension was incubated in fresh serum-free RPMI 1640 with 2 μM CM-H_2DCFDA at 37 °C for 40 min under continuous stirring. The loaded cells were then washed twice with Locke's solution. Then 2×10^6 cells were placed into a cuvette in a thermostatically controlled cell holder at 37 °C and stirred continuously. Fluorescence was excited at 488 nm, and emission was recorded at 530 nm. The change in fluorescence intensity was monitored.

2.5. RT-PCR analysis

Total RNA was extracted from U937 cells using acid guanidinium thiocyanate–phenol–chloroform (Tri-reagent, Cincinnati, OH). One microgram of total RNA was added to 0.5 μg oligo(dT) in diethyl pyrocarbonate-treated water, incubated at 70 °C for 5 min, and then cooled at 4 °C for 5 min. A total of 1 mM concentrations of each of the four dNTPs, 5 μl 5× reverse transcription buffer, and 200 U superscript II reverse transcriptase (Life Technologies) were added, and the reactions were incubated at 42 °C for 1 h and at 75 °C for 10 min and then stored at 4 °C. For PCR amplification, an aliquot of the cDNA synthesis reaction was added to a reaction buffer containing 1 mM dNTPs, 1 mM oligonucleotide primers and 2 U *Taq* DNA polymerase (Promega, Madison, WI). Forty temperature cycles were conducted as follows: denaturation at 95 °C for 1 min; annealing at temperatures specific for each set of primers for 1 min; extension at 72 °C for 1 min in a Minicycler (MJ Research, Watertown, MA). The resultant amplification products were analyzed by agarose gel electrophoresis. The following oligonucleotide primers were used for amplification of H_1R: sense primer, 5′-gccctcgagaccatgagccttcccaattcctc-3′ antisense primer, 5′-cttaagacgtataagcgaggccacccgggcca-3′ (GenBank accession no. NM_000861). We used the primers for TRPC, which is described in previous report [23]. Amplified PCR products were sequenced according to the manufacturer's instructions (Amersham Life Science, Cleveland, OH).

2.6. Measurement of cytosolic Ca^{2+} concentration ($[Ca^{2+}]_i$) and Ca^{2+} imaging

$[Ca^{2+}]_i$ was determined using the fluorescent Ca^{2+} indicator fura-2 as reported previously [13]. Briefly, the cell suspension was incubated in fresh serum-free RPMI 1640 medium with 3 μM fura-2/AM at 37 °C for 60 min with continuous stirring. The loaded cells were then washed twice with Locke's solution. Sulfinpyrazone (250 μM) was added to all solutions to prevent dye leakage. For the fluorometric measurement of $[Ca^{2+}]_i$, 1×10^6 cells/ml were placed into a quartz cuvette in a thermostatically controlled cell holder at 37 °C and continuously stirred. Fluorescence ratios were monitored, with dual excitation at 340 and 380 nm and emission at 500 nm. Calibration of the fluorescent signal in terms of $[Ca^{2+}]_i$ was performed as described by Grynkiewicz et al. [24] using the following equation: $[Ca^{2+}]_i = K_d[R - R_{min}]/(R_{max} - R)](S_{f2}/S_{b2})$, where R is the ratio of fluorescence emitted by excitation at 340 and 380 nm. S_{f2} and S_{b2} are the proportionality coefficients at 380 nm excitation of Ca^{2+}-free fura-2 and Ca^{2+}-saturated fura-2, respectively. To obtain R_{min}, the fluorescence ratios of the cell suspension were measured successively at final concentrations of 4 mM EGTA, 30 mM Trizma base and 0.1% Triton X-100. The cell suspension was then treated with $CaCl_2$ at a final concentration of 4 mM Ca^{2+}, and the fluorescence ratios were measured to obtain the R_{max}. For multiphoton confocal microscopic calcium imaging, 100 nM PMA-induced differentiated U937 cells plated on poly-D-lysine-coated cover slips were pre-loaded with 5 μM Fluo-4/AM dye. After incubation for 30 min at 37 °C, the cells were washed two times with Locke's solution to remove excess dye and examined under the confocal microscope. Groups of U937 cells were selected under the microscope. Measurements of intracellular calcium were performed with the Bio-Rad Radiance 2100 confocal microscope (Bio-Rad Inc.) equipped with a 40× objective (0.75 numerical aperture). The calcium-sensitive Fluo-4 dye was excited by the 488-nm line from an argon laser and the emission fluorescence monitored at 515/30 nm was selected by a band-pass filter. During fluorescence data collection, each scan of a 512 × 512 pixel image took 0.35 s, and the interval between each image scan was ~2 s. Images were stored and processed with laser pix software (Bio-Rad Inc.).

2.7. Mn^{2+} quenching of fura-2 fluorescence

The Mn^{2+} quenching assay was performed as described by Choi et al. [13] to measure the influx of Ca^{2+} from the extracellular space. Briefly, fura-2-loaded cells (5×10^6 cells/ml; described above) were placed into a quartz cuvette in a thermostatically controlled cell holder at 37 °C under continuous stirring. Fluorescence was excited at 360 nm, i.e. the isosbestic wavelength at which Ca^{2+} does not affect fura-2 fluorescence and at which, therefore, changes are caused by Mn^{2+} quenching. Emission was recorded at 500 nm. The potency and slope of the change in fluorescence intensity were recorded after applying 2 mM $MnCl_2$ and the drugs to be tested.

2.8. Analysis of data

All quantitative data are expressed as the mean ± S.E.M. We calculated the IC_{50} with the Microcal Origin for Windows program. Paired *t*-tests were performed for statistical comparisons. Differences were considered significant $^{**}p < 0.01$, $^{***}p < 0.001$.

3. Results

Because of the prominent role of SOCE in shaping the Ca^{2+} response in immune cells [25], we used U937, human promyelocytic cell line. This cell line has served as a good model for the study of Ca^{2+} signaling during inflammatory processes [26]. U937 cells express H1 histamine receptors (H_1Rs), which are important participants in the inflammatory process [27]. This was confirmed by RT-PCR using primers specific for both receptor cDNAs, which yielded amplified products of the expected sizes for H_1R (1.4 kbp) (Fig. 1A, inset). HTMT treatment evoked cytosolic Ca^{2+} increase (Fig. 1A and B) in U937 cells, but HTMT-induced Ca^{2+} entry was not detected. Moreover, the peak levels of $[Ca^{2+}]_i$ rise induced by HTMT were identical in the absence and presence of 2.2 mM extracellular Ca^{2+}. Therefore, we conclude that HTMT-induced signaling does not activate significant amount of extracellular calcium entry.

Since TG is a well-established stimulator of SOCE [28], we next determined whether HTMT inhibits the TG-induced stimulation of SOCE. We found that pretreatment of HTMT significantly attenuated the TG-induced increase in cytosolic Ca^{2+} (Fig. 1A and B) in a concentration-dependent manner, with an IC_{50} of 101 ± 7 μM

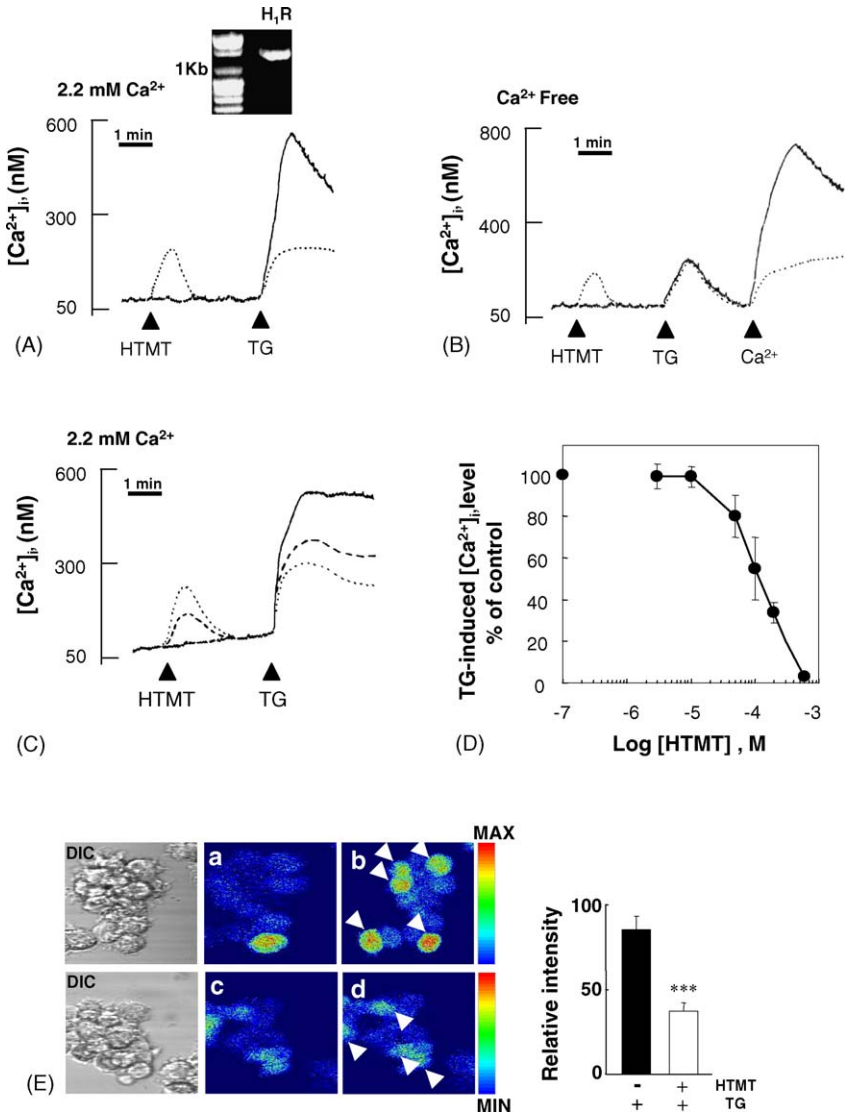

Fig. 1. Effect of HTMT on thapsigargin (TG)-induced SOCE. (A) Fura-2/AM loaded U937 cells were treated with (dotted trace) or without (continuous trace) 100 μM HTMT, then challenged with 1 μM TG. *Inset*: Expression of H_1Rs in U937 cells. Total RNA was extracted from U937 promyelocytes and carried out RT-PCR. (B) The same experiment was performed in the absence of extracellular calcium before the addition of 4 mM $CaCl_2$ (Ca^{2+}). (C) Fura-2/AM loaded HL-60 cells were treated with 100 μM HTMT (dotted trace), 50 μM HTMT (dashed trace) or vehicle (continuous trace), then challenged with 1 μM TG. (D) Concentration-dependent effect of HTMT on TG-induced SOCE in HL-60 cells. Each response stands for maximum value. Each point was obtained from triplicate experiments and is the mean ± S.E.M. (E) The intracellular $[Ca^{2+}]_i$ rise induced by 1 μM TG was measured via multiphoton confocal microscope using calcium sensitive dye Fluo-4/AM. One micromolar PMA induced differentiated U937 cells were stimulated with 1 μM TG in the absence (a and b) or presence (c and d) of 300 μM HTMT. The basal intensity of unstimulated U937 cells are shown in picture (a) and (c). The increase in intensity after 1 μM TG induction is shown in picture (b) (without preincubation of HTMT) and (d) (with preincubation of HTMT). Values represent average fluorescence intensity (region of interest) ± S.E.M. in selected, arrows. $^{***}p < 0.001$ by paired *t*-test.

(Fig. 1D). HTMT blocked TG-induced Ca^{2+} increase not only U937 cells but also HL-60 cells (Fig. 1C). HTMT, however, did not affect TG-induced Ca^{2+} release (Fig. 1B), indicating that the target of HTMT is not the Ca^{2+} store but the SOCE. We also monitored the calcium increase in differentiated U937 cells induced by 100 nM PMA using confocal microscopic calcium imaging (Fig. 1E). Pretreatment of these cells for 5 min with HTMT markedly reduced the fluorescence intensity after application of TG.

To confirm that the store-operated Ca^{2+} current is inhibited in response to application of HTMT, TG-induced store-operated Ca^{2+} current was measured before and after application of HTMT. Fig. 2 shows that TG evoked store-operated Ca^{2+} current, which lasted for nearly 6.5 min (Fig. 2A). Application of HTMT reduced the store-operated Ca^{2+} current to $31.3 \pm 5.1\%$ ($n = 7$) as compared to that in the absence of HTMT (Fig. 2B and C). Therefore, these results indicate that HTMT decreased TG-induced $[Ca^{2+}]_i$ by inhibiting store-operated Ca^{2+} current.

To elucidate the inhibitory effect of HTMT on SOCE, we also tested its effect on TG-induced influx of Ba^{2+} or Mn^{2+} ions, which were added to the extracellular space to monitor Ca^{2+} influx separate from the store-mediated release of intracellular Ca^{2+} (Fig. 3). Ba^{2+} and Mn^{2+} have the additional advantage that they do not generally activate Ca^{2+}-dependent processes, avoiding the possibility of secondarily recruiting Ca^{2+}-activated channels [29]. We found that HTMT inhibited the fluorescence changes induced by Ba^{2+} influx (Fig. 3A) and decreased the rate of fluorescence quenching caused by the binding of cytosolic fura-2 to Mn^{2+} (Fig. 3B and C). Thus, our findings consistently indicate that HTMT targets Ca^{2+} influx through store-operated channels.

We wanted to check the effect of HTMT after the SOCE is established. Besides, we used both HL-60 and U937 cells, two different representative promyelocytic cells, to examine whether the effect of HTMT was general. Like U937 cells, HL-60 cells have also been used as an immune model system to study signaling mechanisms of inflammation. HL-60 cells, TG-induced sustained Ca^{2+} trace was reached in earlier time point rather than U937 cells (Fig. 4A). We found that HTMT inhibited TG-induced sustained cytosolic Ca^{2+} in a concentration-dependent manner (Fig. 4A and B), but histamine (Fig. 4B) and

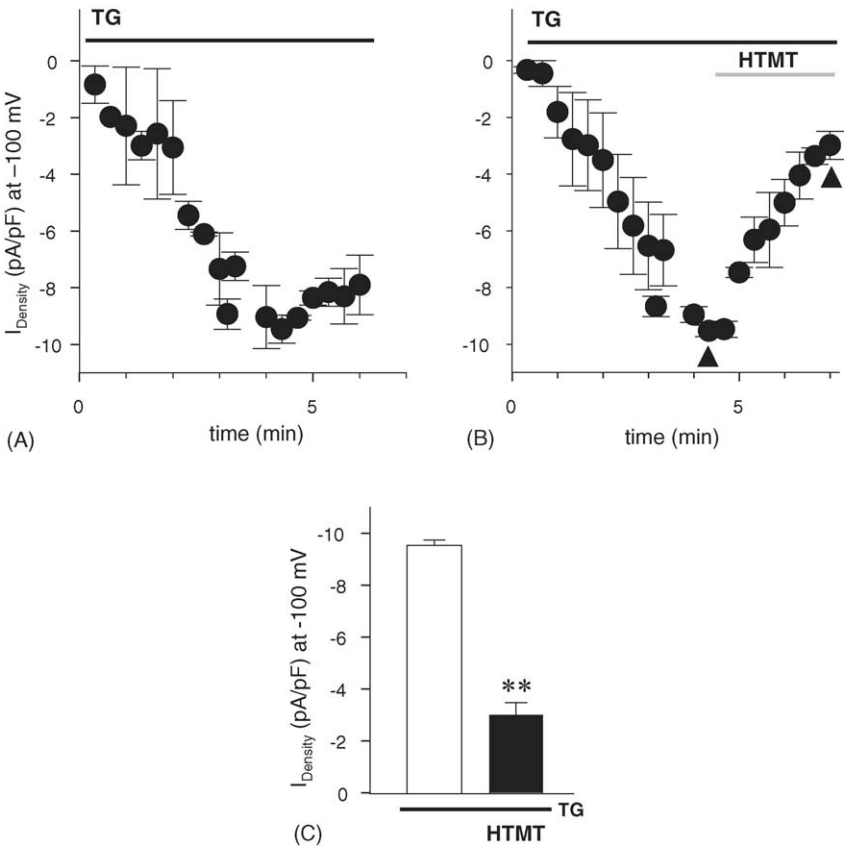

Fig. 2. Effect of HTMT on store-operated Ca^{2+} current in 1 μM PMA-induced differentiated U937 cells. (A) Averaged time courses (mean ± S.E.) of the whole cell currents activated during store depletion in response extracellular thapsigargin (TG, 1 μM) application; currents were measured at −100 mV; time "0" corresponds to the establishment of the whole cell configuration in the event of the beginning of TG exposure. Each point marks applications of 200 ms voltage ramp protocol from the −100 to +100 mV with a 20 s interval. Change in membrane current at −100 mV is plotted as a function of time (min). (B) After application of TG to induce store-operated Ca^{2+} current, HTMT was treated. Application of HTMT was indicated above the current recording. (C) Quantification of the TG-induced store-operated Ca^{2+} current and its inhibition by HTMT. Each current value obtained from panel B indicated by arrows before and after application of HTMT. Experiments were performed four to seven times independently. Data are shown as mean value ± S.E., $^{**}p < 0.01$.

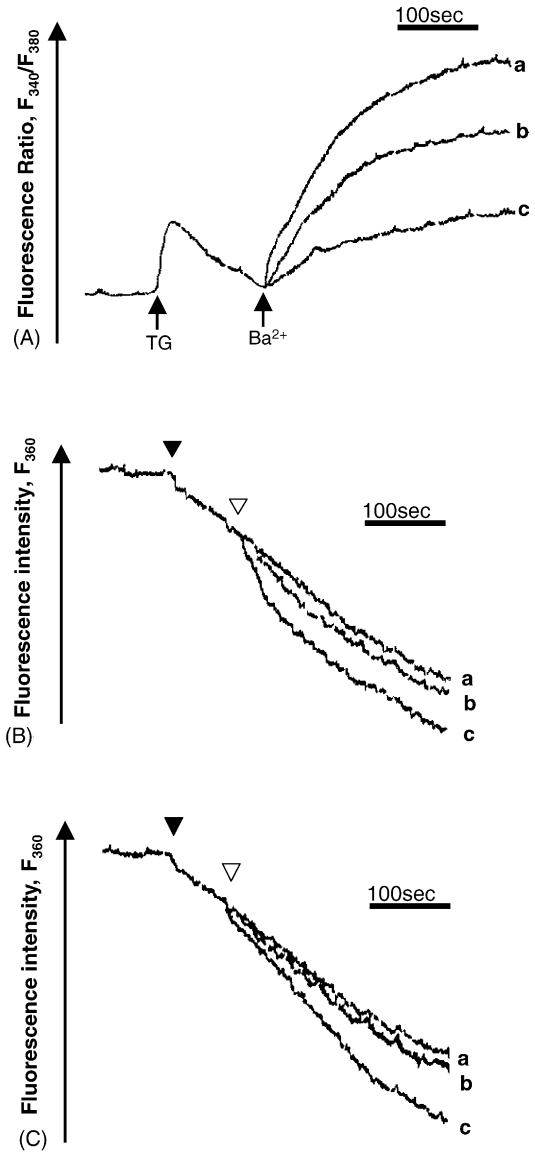

Fig. 3. Effect of HTMT on TG-induced Ba^{2+} and Mn^{2+} influx. (A) Fura-2-loaded U937 cells were stimulated with 1 μM TG with or without the preincubation of cells with HTMT in Ca^{2+}-free medium, then 5 mM Ba^{2+} was added. Stimuli given are as follows: vehicle (a), 100 μM HTMT (b) and 300 μM HTMT (c). The results are depicted as fluorescence ratio of 340 nm and 380 nm (F_{340}/F_{380}). The experiments were independently conducted more than five times. The results were reproducible. Mn^{2+}-induced fura-2 fluorescence quenching was recorded in fura-2/AM-preloaded cells (B: HL-60 cells, C: U937 cells) incubated with 1 mM Mn^{2+} (dark arrow head) and drugs at the indicated point (open arrow head). Stimuli given are as follows: vehicle (a), 1 μM TG with 300 μM HTMT (b) and 1 μM TG (c). The influx of Mn^{2+} was measured as described in Section 2. The results are depicted as fluorescence intensities at 360 nm (F_{360}). The data presented are representative of four independent experiments.

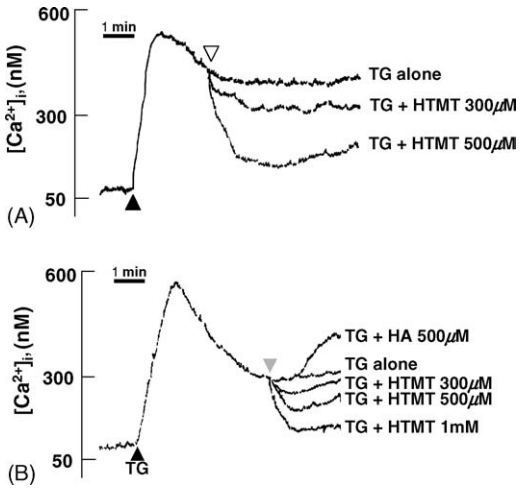

Fig. 4. Effect of 2-APB on the HTMT action in the inhibition of TG-induced SOCE. (A) Fura-2-loaded HL-60 cells were treated with 1 μM TG and then challenged with indicated concentration of HTMT. (B) Fura-2-loaded U937 cells were treated with 1 μM TG and then challenged with indicated concentration of histamine (HA) and HTMT. The presented data are representative of more than five independent experiments.

maleate salt (data not shown) did not. Strangely, 500 μM histamine enhanced TG-induced sustained Ca^{2+} trace (Fig. 4B).

To confirm that H_1R activation is not involved in the inhibition of SOCE, we stimulated H_1Rs with their selective agonists, 2-methylhistamine and 2-thiazolylethylamine [30]. Neither of these, however, reduced TG-induced calcium influx (Fig. 5A and B). To further confirm the response, we checked HTMT effect on TG-induced Ca^{2+} increase in C6 mouse glial cells. In C6 glioma cells, however, there was no detectable $[Ca^{2+}]_i$ rise in response to HTMT, indicating that C6 cells do not express HTMT-responsive receptors. We also tested HTMT's effect in bovine adrenal chromaffin cells, which express H1 receptors responsive to histamine, but there was no Ca^{2+} response by HTMT treatment (data not shown). These results suggest that HTMT's effect on Ca^{2+} rise might be highly immune cell-selective. Mepyramine, a H1 receptor antagonist, was pretreated then checked HTMT's effect on TG-induced Ca^{2+} entry. As shown in Fig. 6, we could not find any significant recovery. These results indicating that HTMT acts directly on SOCE rather than on H_1R activation and its downstream signaling cascade.

Since superoxide production is a marker for inflammatory processes in leukocytes [31], we tested the effects of HTMT on SOCE-induced superoxide production in HL-60 cells differentiated with all-*trans* retinoic acid (Fig. 7A). In previous report [32], intracellular calcium concentration and O_2^- production is tightly linked. Since the HTMT could increase small amount of intrecellular calcium concentration in HL-60 cells, HTMT itself may exert O_2^- production. For that reason, we induced cytosolic Ca^{2+} by TG treatment in the presence or absence of HTMT. First, 60 min incubation with TG only increased the large amount of superoxide in the extracellular space (Fig. 7A). Besides, HTMT only also induce O_2^- production (Fig. 7A), indicating that HTMT-induced Ca^{2+} response is related with O_2^- production. Although HTMT generated superoxide, HTMT's attenuating effect on TG-induced O_2^- formation was predominant in our experimental conditions (Fig. 7A). CM-H_2DCFDA loaded U937

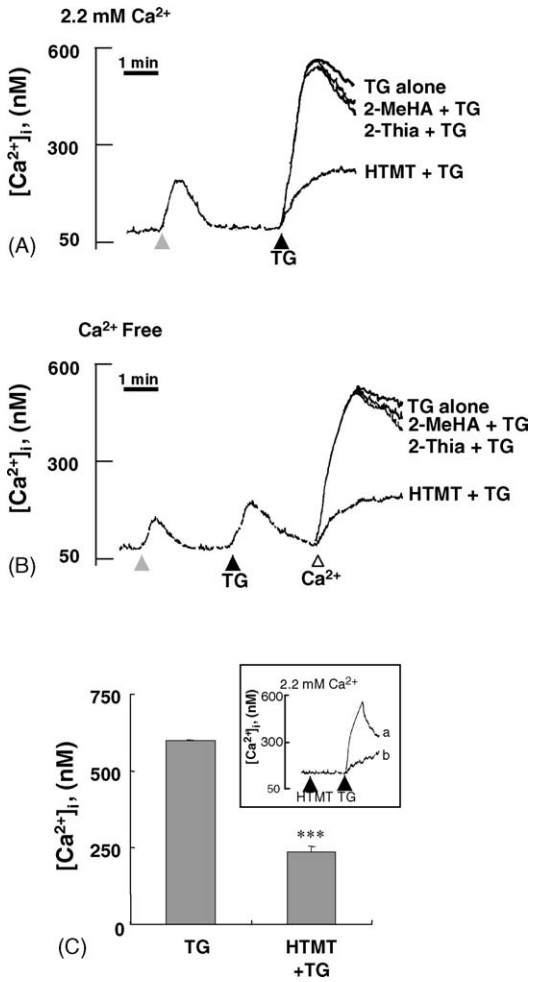

Fig. 5. Selective action of HTMT on SOCE. Effect of H_1R specific agonist on TG-induced Ca^{2+} influx. One hundred micromolar HTMT, 100 μM 2-thiazolylethylamine (2-Thia) or 100 μM 2-methylhistamine (2-MeHA) was pretreated 3 min before TG treatment in the presence (A) or absence (B) of 2.2 mM extracellular Ca^{2+}. (C) Effect of HTMT on TG-induced Ca^{2+} increase in C6 mouse glial cell line. *Inset*: Representative Ca^{2+} increase trace of 1 μM TG treatment without HTMT (trace, a) or with HTMT (trace, b). The experiment was performed three times independently. $^{***}p < 0.001$ by paired *t*-test.

cells also showed TG-induced superoxide generation and inhibited by HTMT pretreatment (Fig. 7B). Since, we observed the inhibitory effect of HTMT on the SOCE in both HL-60 cells and U937 cells, we designed to check its effect and get results from both cell systems. In both assays, similar results were obtained from both of the cells, although the extent of inhibition was not exactly the same. We thus decided to present more clear results. Taken together, these results suggest that HTMT inhibits superoxide production by blocking SOCE.

4. Discussion

Increases in the cytosolic free calcium concentration ($[Ca^{2+}]_i$) act as a powerful stimulus for various physiological responses in virtually all cell types [33]. $[Ca^{2+}]_i$ is

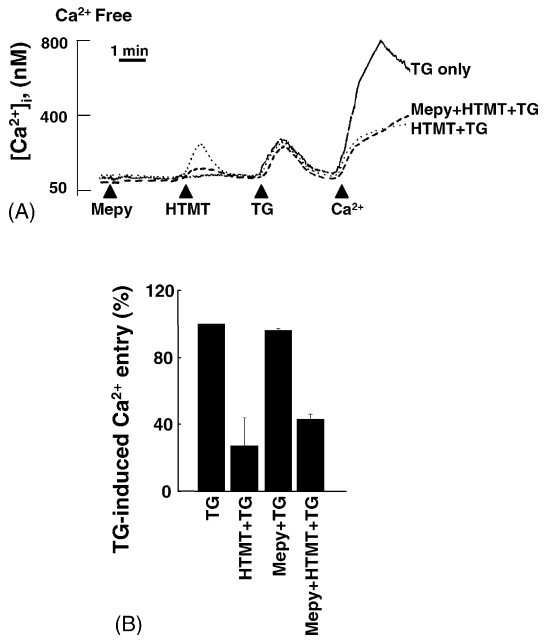

Fig. 6. Effect of mepyramine on HTMT's SOCE blocking. (A) Fura-2-loaded U937 cells were stimulated with 1 μM TG with or without the preincubation of cells with HTMT in Ca^{2+}-free medium, then 2.2 mM Ca^{2+} was added. Continuous trace stands for TG only, dotted trace shows the effect of HTMT on TG-induced Ca^{2+} entry, dashed trace represents the effect of mepyramine on HTMT- and TG-induced response. (B) Each bar indicates the data obtained from quantification of panel A. Each point was obtained from triplicate experiments and is the mean ± S.E.M.

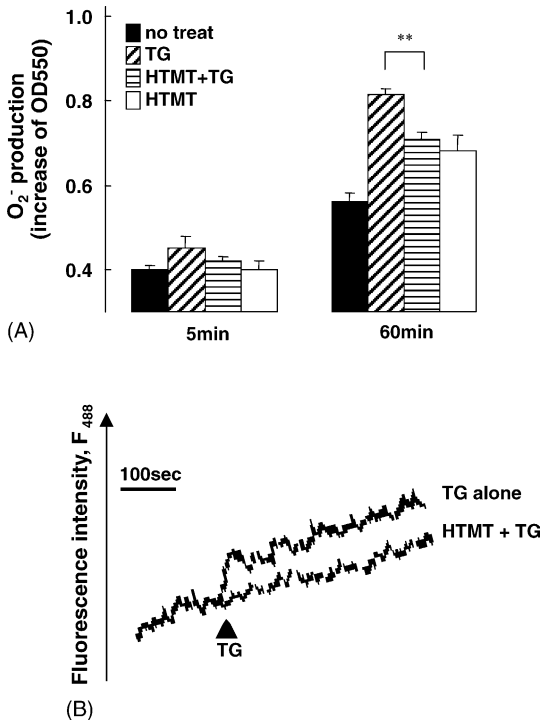

Fig. 7. Effects of HTMT on SOCE-induced superoxide production. (A) Granulocytic differentiated HL-60 cells (by 1 μM trans-RA) were preincubated with or without 300 μM HTMT for 3 min, then treated with 1 μM TG for 5 and 60 min. Each result is the mean ± S.E.M. of triplicate assays. $^{**}p < 0.01$ vs. TG treatment. (B) CM-H_2DCFDA-loaded U937 cells were preincubated with or without 300 μM HTMT then treated with 1 μM TG. Superoxide formation was measured as described in Section 2.

involved in regulating the host defense activity of resident cells such as macrophages and mast cells, as well as eosinophils, lymphocytes and neutrophils, which migrate to the lungs during inflammation and infection [34]. In leucocytes, $[Ca^{2+}]_i$ plays a critical role in determining cellular responsiveness to inflammatory stimuli by regulating a variety of functional responses, including degranulation, lipid mediator release, superoxide anion generation and cell proliferation [6,7]. Ca^{2+} influx through store-operated calcium channels is also functionally important in non-excitable cells [35], but the channels have not been successfully exploited as the targets for anti-inflammatory therapy. A new generation of store-operated calcium channel antagonists may find a role in the treatment of inflammatory responses. In recent years, much attention has focused on the mechanism of SOCE [36]. SOCE is thought to be a major regulator of immune responses, including O_2^- production in granulocytic differentiated HL-60 cells [37] and neutrophils [38], IL-8 release in neutrophils [39], histamine release in mast cells [40] and platelet aggregation [41]. It has been reported that the PAF-induced priming of neutrophils requires Ca^{2+} influx [42], which has been found to be SOCE [43].

In present study, we have shown that TG-induced SOCE is inhibited by HTMT. This finding was clearly supported by our results: (1) HTMT did not inhibit TG-induced Ca^{2+} release from internal stores in the absence of external Ca^{2+} (Fig. 1B), (2) HTMT also inhibited TG-induced sustained Ca^{2+} elevation not only in U937 and HL-60 cells (Fig. 4A and B) but also in C6 glial cells (Fig. 5C) which are not responsive to HTMT pretreatment. (3) HTMT inhibited TG-induced Ba^{2+} influx (Fig. 3A) and fluorescence quenching with Mn^{2+} influx (Fig. 3B and C) and (4) HTMT act on SOCE similar with 2-APB (Fig. 4C and D).

Interestingly, HTMT acts to attenuate the inflammatory responses of immune cells [15], in addition to its effect on histamine receptors. Our findings suggest that the HTMT effect is of the non-H_1Rs-mediated pathway because of its high effective concentration needed for the effect (Fig. 1D). Since neither 2-methylhistamine nor 2-thiazolylethylamine, potent and selective H_1R agonists, inhibited SOCE (Fig. 5A and B), the effects of HTMT may occur through its direct interaction with membrane proteins or channels. In addition, we tested the effect of HTMT-induced H_1R signaling on SOCE by using U73122 (PLC inhibitor) and mepyramine (H1 receptor antagonist), but we could not find any significant recovery. Furthermore, histamine (Fig. 4B) and maleate salt (data not shown) had no effect on the TG-induced calcium influx, demonstrating that H_1R-mediated intracellular signaling is not involved in the HTMT's effect on the SOCE. As shown in Fig. 4B, histamine enhanced TG-induced SOCE sustain Ca^{2+} trace. Usually, histamine activates not only H1 receptors, but H2 receptors. For this reason, H2 receptor-mediated signaling may activate its effector enzyme, adenylyl cyclase and cAMP generated from the effector enzyme activates protein kinase A (PKA). According to previous report [46], activated PKA induced by H2 signaling may enhanced thapsigargin-induced Ca^{2+} entry, indicating that histamine is capable to induce a further increase in $[Ca^{2+}]_i$. We, therefore, postulate that the trifluoromethylphenyl heptanecarboxamide group of HTMT may be the critical functional moiety in its effect on SOCE. This clarifies that we have identified a new chemical class of SOCE blockers.

Increasing evidence suggests a pivotal role of reactive oxygen species (ROS) in human pathophysiology [44]. Although oxidative stress and intracellular free Ca^{2+} are involved in various diseases, the regulatory mechanism of Ca^{2+}-induced ROS generation has not yet been well defined. We could find TRPC2, TRPC5 and TRPC6 in U937 cells by RT-PCR analysis (data not shown) [23]. In previous report, experiments with TRPC species overexpressed in HEK293 cells confirmed that TRPC3 and TRPC4 are able to form redox sensitive cation channels [45]. In addition, oxidative stress-induced disruption of caveolin 1-rich lipid raft domains, which interfere with functional TRPC channels, is likely to contribute to redox modulation of TRP proteins and to oxidative stress-induced changes in cellular Ca^{2+} signaling [45]. According to our data, negative regulation of TRPC by HTMT (Fig. 6) also could be another important aspect in the alleviation of ROS and inflammation in immune system. Thus, modulation of these cellular redox pathway by HTMT may offer unique opportunities for therapeutic interventions. Importantly, our results indicate that this novel function of HTMT may also be a useful tool for investigating SOCE and its effects on the inflammation and autoimmune diseases. The ability of HTMT to inhibit SOCE suggests its potential use as a lead compound for the design of anti-inflammatory drugs.

Acknowledgements

We thanks to GlaxoSmithKline (Miss Lorraine Bray) Inc. for providing 2-methylhistamine and 2-thiazolylethylamine. This work was supported by the Frontier Research Project of the POSCO, Brain Korea 21 Program of the Korean Ministry of Education and BioGreen 21 program (Code# 20050401034641) of the Korean Rural Development Administration and the Brain Neurobiology Research Program (M10412000088-04N1200-08810).

References

[1] Swain SD, Rohn TT, Quinn MT. Neutrophil priming in host defense: role of oxidants as priming agents. Antioxid Redox Signal 2002;4(1):69–83.

[2] Li SW, Westwick J, Poll CT. Receptor-operated Ca^{2+} influx channels in leukocytes: a therapeutic target? Trends Pharmacol Sci 2002;23(2):63–70.

[3] Bielefeldt K, Whiteis CA, Sharma RV, Abboud FM, Conklin JL. Reactive oxygen species and calcium homeostasis in cultured human intestinal smooth muscle cells. Am J Physiol 1997;272(6 Pt 1):G1439–50.
[4] Streb H, Irvine RF, Berridge MJ, Schulz I. Release of Ca^{2+} from a nonmitochondrial intracellular store in pancreatic acinar cells by inositol-1,4,5-trisphosphate. Nature 1983;306(5938):67–9.
[5] Penner R, Fleig A. Store-operated calcium entry: a tough nut to CRAC. Sci STKE 2004;2004(243):38.
[6] Wu X, Zagranichnaya TK, Gurda GT, Eves EM, Villereal ML. A TRPC1/TRPC3-mediated increase in store-operated calcium entry is required for differentiation of H19-7 hippocampal neuronal cells. J Biol Chem 2004;279(42):43392–402.
[7] Vanden Abeele F, Skryma R, Shuba Y, Van Coppenolle F, Slomianny C, Roudbaraki M, et al. Bcl-2-dependent modulation of Ca(2+) homeostasis and store-operated channels in prostate cancer cells. Cancer Cell 2002;1(2):169–79.
[8] Suzuki Y, Yoshimaru T, Matsui T, Inoue T, Niide O, Nunomura S, et al. Fc epsilon RI signaling of mast cells activates intracellular production of hydrogen peroxide: role in the regulation of calcium signals. J Immunol 2003;171(11):6119–27.
[9] Tran QK, Ohashi K, Watanabe H. Calcium signalling in endothelial cells. Cardiovasc Res 2000;48(1):13–22.
[10] Mattson MP, LaFerla FM, Chan SL, Leissring MA, Shepel PN, Geiger JD. Calcium signaling in the ER: its role in neuronal plasticity and neurodegenerative disorders. Trends Neurosci 2000;23(5): 222–9.
[11] Nishida M, Sugimoto K, Hara Y, Mori E, Morii T, Kurosaki T, et al. Amplification of receptor signalling by Ca^{2+} entry-mediated translocation and activation of PLCgamma2 in B lymphocytes. Embo J 2003;22(18):4677–88.
[12] Fanger CM, Hoth M, Crabtree GR, Lewis RS. Characterization of T cell mutants with defects in capacitative calcium entry: genetic evidence for the physiological roles of CRAC channels. J Cell Biol 1995;131(3):655–67.
[13] Choi SY, Ha H, Kim KT. Capsaicin inhibits platelet-activating factor-induced cytosolic Ca^{2+} rise and superoxide production. J Immunol 2000;165(7):3992–8.
[14] Wang JP, Tseng CS, Sun SP, Chen YS, Tsai CR, Hsu MF. Capsaicin stimulates the non-store-operated Ca(2+) entry but inhibits the store-operated Ca(2+) entry in neutrophils. Toxicol Appl Pharmacol 2005.
[15] Qiu R, Melmon KL, Khan MM. Effects of lymphokines and mitogens on a histamine derivative-induced intracellular calcium mobilization and inositol phosphate production. Biochem Pharmacol 1994;47(11): 2097–103.
[16] De Man JG, Moreels TG, De Winter BY, Bogers JJ, Van Marck EA, Herman AG, et al. Disturbance of the prejunctional modulation of cholinergic neurotransmission during chronic granulomatous inflammation of the mouse ileum. Br J Pharmacol 2001;133(5): 695–707.
[17] Levy R, Rotrosen D, Nagauker O, Leto TL, Malech HL. Induction of the respiratory burst in HL-60 cells. Correlation of function and protein expression. J Immunol 1990;145(8):2595–601.
[18] Withnall MT, Pennington A, Wiseman D. Characterisation of cytosolic phospholipase A2 as mediator of the enhanced arachidonic acid release from dimethyl sulphoxide differentiated U937 cells. Biochem Pharmacol 1995;50(11):1893–902.
[19] Wang Z, Su ZZ, Fisher PB, Wang S, VanTuyle G, Grant S. Evidence of a functional role for the cyclin-dependent kinase inhibitor p21(WAF1/CIP1/MDA6) in the reciprocal regulation of PKC activator-induced apoptosis and differentation in human myelomonocytic leukemia cells. Exp Cell Res 1998;244(1):105–16.
[20] Elbling L, Weiss RM, Teufelhofer O, Uhl M, Knasmueller S, Schulte-Hermann R, et al. Green tea extract and (−)-epigallocatechin-3-gallate, the major tea catechin, exert oxidant but lack antioxidant activities. FASEB J 2005.
[21] Cohen HJ, Chovaniec ME. Superoxide generation by digitonin-stimulated guinea pig granulocytes. A basis for a continuous assay for monitoring superoxide production and for the study of the activation of the generating system. J Clin Invest 1978;61(4):1081–7.
[22] Witenberg B, Kalir HH, Raviv Z, Kletter Y, Kravtsov V, Fabian I. Inhibition by ascorbic acid of apoptosis induced by oxidative stress in HL-60 myeloid leukemia cells. Biochem Pharmacol 1999;57(7): 823–32.
[23] Babich LG, Ku CY, Young HW, Huang H, Blackburn MR, Sanborn BM. Expression of capacitative calcium TrpC proteins in rat myometrium during pregnancy. Biol Reprod 2004;70(4):919–24.
[24] Grynkiewicz G, Poenie M, Tsien RY. A new generation of Ca^{2+} indicators with greatly improved fluorescence properties. J Biol Chem 1985;260(6):3440–50.
[25] Heiner I, Eisfeld J, Luckhoff A. Role and regulation of TRP channels in neutrophil granulocytes. Cell Calcium 2003;33(5–6):533–40.
[26] Kanellis J, Bick R, Garcia G, Truong L, Tsao CC, Etemadmoghadam D, et al. Stanniocalcin-1, an inhibitor of macrophage chemotaxis and chemokinesis. Am J Physiol Renal Physiol 2004;286(2):F356–62.
[27] Wang KY, Arima N, Higuchi S, Shimajiri S, Tanimoto A, Murata Y, et al. Switch of histamine receptor expression from H2 to H1 during differentiation of monocytes into macrophages. FEBS Lett 2000;473(3):345–8.
[28] Zagranichnaya TK, Wu X, Villereal ML. Endogenous TRPC1, TRPC3 and TRPC7 proteins combine to form native store-operated channels in HEK-293 cells. J Biol Chem 2005.
[29] Putney Jr JW. Store-operated calcium channels: how do we measure them and why do we care? Sci STKE 2004;2004(243):37.
[30] Kamei C. Involvement of central histamine in amygdaloid kindled seizures in rats. Behav Brain Res 2001;124(2):243–50.
[31] Forman HJ, Torres M. Reactive oxygen species and cell signaling: respiratory burst in macrophage signalling. Am J Respir Crit Care Med 2002;166(12 Pt 2):S4–8.
[32] Valentin F, Bueb J, Capdeville-Atkinson C, Tschirhart E. Rac-1-mediated O_2-secretion requires Ca^{2+} influx in neutrophil-like HL-60 cells. Cell Calcium 2001;29(6):409–15.
[33] Spassova MA, Soboloff J, He LP, Hewavitharana T, Xu W, Venkatachalam K, et al. Calcium entry mediated by SOCs and TRP channels: variations and enigma. Biochim Biophys Acta 2004;1742(1–3):9–20.
[34] Niggli V. Signaling to migration in neutrophils: importance of localized pathways. Int J Biochem Cell Biol 2003;35(12):1619–38.
[35] Elliott AC. Recent developments in non-excitable cell calcium entry. Cell Calcium 2001;30(2):73–93.
[36] Strubing C, Krapivinsky G, Krapivinsky L, Clapham DE. TRPC1 and TRPC5 form a novel cation channel in mammalian brain. Neuron 2001;29(3):645–55.
[37] Merritt JE, Armstrong WP, Benham CD, Hallam TJ, Jacob R, Jaxa-Chamiec A, et al. SK&F 96365, a novel inhibitor of receptor-mediated calcium entry. Biochem J 1990;271(2):515–22.
[38] Kuhns DB, Young HA, Gallin EK, Gallin JI. Ca^{2+}-dependent production and release of IL-8 in human neutrophils. J Immunol 1998; 161(8):4332–9.
[39] Lloret S, Moreno JJ. Ca^{2+} influx, phosphoinositide hydrolysis, and histamine release induced by lysophosphatidylserine in mast cells. J Cell Physiol 1995;165(1):89–95.
[40] Huang SJ, Kwan CY. Cyclopiazonic acid and thapsigargin induce platelet aggregation resulting from Ca^{2+} influx through Ca^{2+} store-activated Ca^{2+}-channels. Eur J Pharmacol 1998;341(2–3): 343–7.
[41] Walker BA, Hagenlocker BE, Ward PA. Superoxide responses to formyl-methionyl-leucyl-phenylalanine in primed neutrophils. Role of intracellular and extracellular calcium. J Immunol 1991;146(9): 3124–31.
[42] Biro T, Maurer M, Modarres S, Lewin NE, Brodie C, Acs G, et al. Characterization of functional vanilloid receptors expressed by mast cells. Blood 1998;91(4):1332–40.
[43] Elzi DJ, Hiester AA, Silliman CC. Receptor-mediated calcium entry is required for maximal effects of platelet activating factor primed

responses in human neutrophils. Biochem Biophys Res Commun 1997;240(3):763–5.

[44] Manton KG, Volovik S, Kulminski A. ROS effects on neurodegeneration in Alzheimer's disease and related disorders: on environmental stresses of ionizing radiation. Curr Alzheimer Res 2004;1(4): 277–93.

[45] Groschner K, Rosker C, Lukas M. Role of TRP channels in oxidative stress. Novartis Found Symp 2004;258:222–30 [discussion 231–5, 263–6].

[46] Song SK, Choi SY, Kim KT. Opposing effects of protein kinase A and C on capacitative calcium entry into HL-60 promyelocytes. Biochem Pharmacol 1998;56(5):561–7.